Magnetic Properties of Pure Iron for the Upgrade of the LHC Superconducting Dipole and Quadrupole Magnets

Magnetic properties of pure iron for the upgrade of the LHC superconducting dipole and quadrupole magnets

P. Arpaia[1,2], M. Buzio[2], A. Liccardo[1], A. Parrella[1,2,3], M. Pentella[1,2], R. Principe[2] and P.M. Ramos[3]
[1]Department of Electrical Engineering and Information Technology, University of Naples Federico II, Naples, Italy
[2]CERN, Geneva, Switzerland
[3]Instituto Superior Técnico, Instituto de Telecomunicações, University of Lisbon, Lisbon, Portugal

The construction of the superconducting magnets for the High-Luminosity upgrade of the LHC accelerator at CERN has resulted in demands for 1800 tonnes of ferromagnetic laminations for the magnet iron yokes. The magnetic properties of the selected steel, ARMCO® Pure Iron, have been measured, within annealing treatment sequences from 750 °C to 850 °C, at operation temperatures of 4 K to 300 K. It is shown that annealing treatment improves the magnetic performance of the material, if the material is kept at room temperature. However, this improvement disappears after cooling down the material to the operation conditions of 4 K. The dependency on the operation temperature was shown by testing the material at the cryogenic temperature of roughly 4 K, 77 K and at room temperature. The magnetic performance the material shown at room temperature have not been found at cryogenic temperatures. Nevertheless, the results obtained are still acceptable in comparison to the properties of the alternative materials. Tests performed before and after the application of a mechanical stress have also been studied to validate the production process.

***Index Terms*—Magnetic properties, Pure iron, Electromagnets, Cryogenic measurements, High-Luminosity LHC**

I. Introduction

THE High Luminosity Large Hadron Collider (HL-LHC) is a project to upgrade the LHC to maintain scientific progress and exploit the LHC's full capacity [1]. By increasing its peak luminosity by a factor of five over nominal value, it will be possible to reach a higher level of integrated luminosity, nearly ten times the initial LHC design target. New magnets in the insertion region and stronger dipole magnets in the dispersion suppression region will be installed in order to make space for additional collimators. The nominal magnetic field of the dipole magnets will increase from 8.6 T to 11 T [2].

In the past, a low-carbon steel, known under the trade name MAGNETIL BL™ and produced by Cockerill Sambre-ARCELOR Group [3], has been used for the production of the iron yoke laminations of the LHC main magnets. The magnetic characterization of this material is described in [4], [5]. This would have been the ideal choice also for the new HL-LHC magnets, if it had still been available at the moment of the tender. Instead, ARMCO® Pure Iron Grade 4 produced by AK Steel has been chosen due to its high purity and magnetic performance. This paper reports the three years of activity concerning the procurement, production and magnetic and mechanical characterization of 1800 tonnes of ARMCO® Pure Iron, to be used mainly for the single aperture Nb_3Sn quadrupole magnets (inner triplet) MQXF [6] and 11 T Nb_3Sn dipole magnets [7].

II. ARMCO® pure iron for HL-LHC

For the production of the iron yoke laminations, the ARMCO® Pure Iron is the steel grade that better corresponds to the CERN requirements as defined in the technical specification IT4009 [8]. ARMCO® Pure Iron is low carbon steel that undergoes purification during melting by using special refining techniques. After solidification, it has a particularly homogeneous composition with regard to the impurity distribution. In the grade 4 version, ARMCO® Pure Iron presents a maximum carbon content lower than 0.003% and very low values of oxygen, sulfur, nitrogen and cobalt. Due to the low carbon content, the microstructure consists of 100% ferrite. Although, with existing technology, the carbon content has never exceeded 0.0023% with an average value of 0.0013% in the last years production.

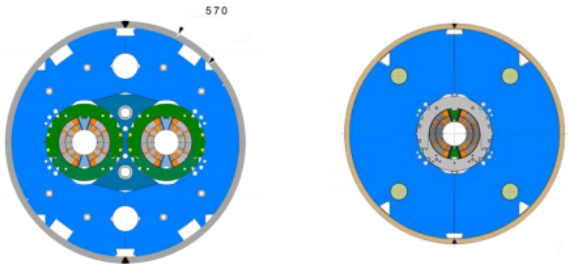

Fig. 1. Cross-section of the two-in-one aperture MBH (left), and the single aperture MBH (left). In blue the yoke.

The ARMCO® Pure Iron has a minimum Fe content of 99.85 weight%, hot rolled at 800 °C, cooled in air (not water cooled in line), with pickling and oiling of the metal sheets for rust protection. It is a non-ageing type, delivered in sheets, which are 4000 mm long and 750 mm wide. They are conditioned in 4-ton packs for the transport and storage. The sheets thickness is 5.8 mm, which is a standard value for the yoke laminations used for the construction of the LHC Main Bending and Quadrupole Magnets. Due to its microstructure, the ARMCO® Pure Iron has only marginal mechanical properties. Although it was selected to match

with the magnetic specification, the grade presents adequate mechanical characteristics (not too brittle at low temperature). For the steel sheets, CERN accepts material with a grain size ASTM lower than 6, corresponding to an ultimate tensile strength around 300 MPa and a yield strength around 180 MPa.

III. Magnetic properties

A. Samples and experimental method

Test samples have been machined out of the coils during the sheet cutting process. In order not to alter the magnetic properties of the steel, these samples have been cut at very low speed. A water jet cutting method, with abrasive powder, combined with a slow machining to obtain the required tolerances has been employed. Punching of the rings is not permitted. The samples were obtained as rings (outer diameter 114 *mm* ± 0.05 *mm*, inner diameter 76 *mm* ± 0.05 *mm*, thickness 15 *mm* ± 0.05 *mm*). The results presented here refer to two groups of samples. The former consists of 5 samples annealed as summarized in Tab. I and tested to investigate the role of annealing and cryogenic temperatures. The latter consists of three samples with the same annealing tested before and after the application of a cold work to investigate its role on the magnetic properties. AK steel provides the heat treatment guidelines for the annealing. In detail, the annealing parameters are: heating rate of 2-4 °C/min, a hold temperature of 820 °C for 60 min, with an additional 15 minutes for each 0.5 cm thickness over 2.5 cm and a cooling rate of 2-4 °C/min until the parts are below 550-600 °C. The samples were tested under quasi-static conditions. The normal magnetization curve, the hysteresis loop, and the relative magnetic permeability curve have been measured by means of a measurement system developed at CERN based on the flux-metric method of the international standard IEC 60404-4 [9]. The detailed discussion on the measurement principles involved is given in [10].

TABLE I
Summary of the thermal treatment on the samples

#	Reference	Weight [g]	Annealing time [°C]	Annealing time [h]
1	A	812	Not Annealed	0
2	B	815	750	1
3	C	816	750	5
4	D	816	850	1
5	E	816	850	5
6	A25112-4	256	750	1
7	A25112-3	257	750	1
8	A25114-4	256	750	1

B. Effects of the annealing on magnetic properties

The five samples of ARMCO pure iron summarized in Tab. I have been magnetically tested at CERN to asses their magnetic properties. The tests aimed at obtaining the B-H curve for all the samples, to check (i) the magnetic properties of the material for different heating annealing, and (ii) that the magnetic properties of the material are suitable for the LHC magnet construction requirements (IT4009 specification). All the samples were tested at room temperature.

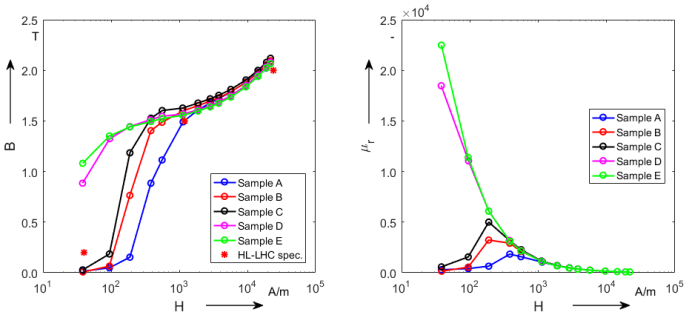

Fig. 2. B-H (left) and relative permeability (right) curves for the five ring samples and the LHC specifications.

TABLE II
Summary of test results of the samples

Sample	A	B	C	D	E	LHC
H [A/m]	B [T]	B [T]	B [T]	B [T]	B [T]	B [T]
40	0.01	0.01	0.03	0.89	1.08	0.20
1200	1.49	1.59	1.63	1.56	1.56	1.50
24000	2.02	2.06	2.08	2.03	2.02	2.00

The results shown in Fig. 2 are from two different sets of measurements: the former for magnetic fields from 40 to 700 A/m, the latter from 700 to 22000 A/m. This is to optimize the accuracy of the obtained B-H curves, since at low fields a lower ramp rate is required. In Table II, the values of the measured flux density B on the samples, at a given value of the magnetic field H, are compared with LHC specifications. The initial specifications are matched by all the samples for magnetic fields higher than 1200 A/m. However, at 40 A/m only samples D and E have shown a corresponding flux density value higher than the CERN threshold of 0.2 T. This is clearly a consequence of the annealing treatment at 850 °C, as increasing the annealing temperature means relaxing the residual stress. Fig 2 indicates the large increase of maximum permeability after the final treatment at 850 °C for 5 hours. Permeability is very sensitive to residual stresses, because these impose constraints on the degrees of freedom of the domain structure, thereby engendering the rise of demagnetization fields at the grain boundaries [11]. The reasoning behind the application of an annealing process is to increase both the magnetic and the mechanical properties. Annealing influences the domain's movement, which depends on the grain size, the micro-structure and the impurity's distribution. Furthermore, the more stressful the treatment is (high temperatures, long times of persistences at high temperatures, etc.), the higher is the influence on the magnetic properties, specially at low fields. It is noted that these differences at low fields disappear around the knee of the curve, where the magnetization rotations enter into play. Hence, in this region the effects of the annealing treatment are meaningless because the effect of the saturation's magnetization predominant. Here, the magnetization process proceeds by rotations and the crystallographic texture remains the sole important structural property [12].

C. Effects of the operation temperature on magnetic properties

Since sample E has shown the highest magnetization properties, it has also been tested at cryogenic temperatures, being the right candidate to replace MAGNETIL BL^{TM}. The aim of this test is to assess the operation performance of the material. Fig. 3 shows the influence of the operation temperature on the initial magnetization and permeability curves. Specifically, the figure displays three initial magnetization curves at 300 K, 77 K and 4.2 K. A significant decrease of the material magnetic softening is observed when the temperature drops from 300 K to 77 K. A less significant but still appreciable decrease is observed from 77 K to 4.2 K. Cooling to cryogenic temperatures results in harder magnetic properties. This can be explained with a model of domain wall motion inhibited by inclusions. As for the annealing, it is noted that the differences observed at low fields disappear around the knee of the B-H curve. This means that at operation temperature the material shows a lower value of maximum relative permeability, but does not change the saturation.

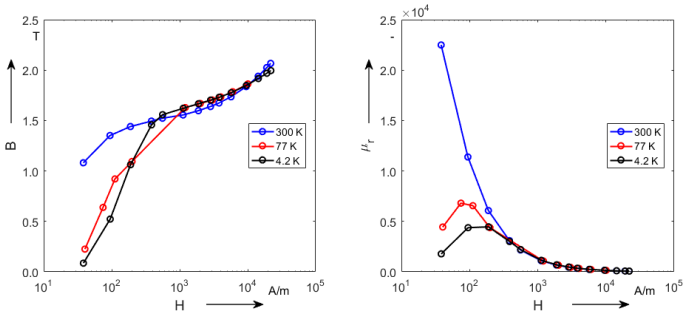

Fig. 3. Initial magnetization curves and relative magnetic permeability of sample E at 300 K, 77 K and 4.2 K

D. Ageing effects on the magnetic properties

After roughly three years from the first tests, a second campaign of measurements was performed on the same samples (except sample D) to verify their stability and the effects of ageing. Fig. 4 and Fig. 5 show the results of these new tests.

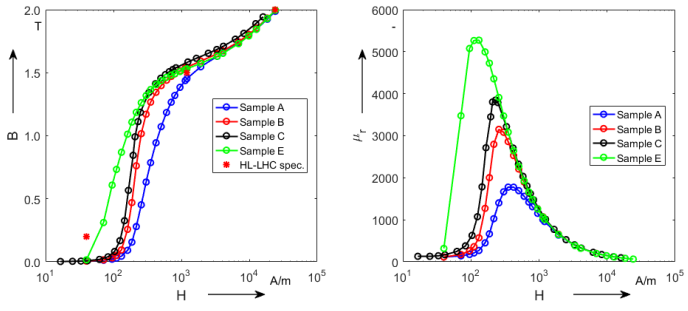

Fig. 4. Results of the recent campaign measurements.

Surprisingly, sample E shows a severe degradation of its magnetic softening, specially at low fields, its magnetic permeability peak going from higher than 22000 to less than 6000, while all the other samples show more or less the same magnetic properties shown in the previous study. This behavior cannot be explained by the ageing of the material. Showing better magnetic properties than the others, sample E was selected for further tests at cryogenic temperatures, hence sample E is the only sample that was dipped in a cryogenic thermal bath after the initial tests. In Section III-C, the degradation of the magnetic properties due to a thermal cycle is shown. The strong degradation shown by sample E in Fig. 5 is due to the fact that the material was cooled down to 4.2 K in a fast way and, after the measurements, brought back to room temperature fast as well. These fast changes in temperature may have generated some internal strains which is the cause of sample E magnetic properties degradation. At cryogenic temperatures this effect should exist as well, although, the low temperature effects are predominant respect to the effect of the strain. In the saturation regions the effect is negligible because the behavior of the material in this region is dominated by the magnetization saturation.

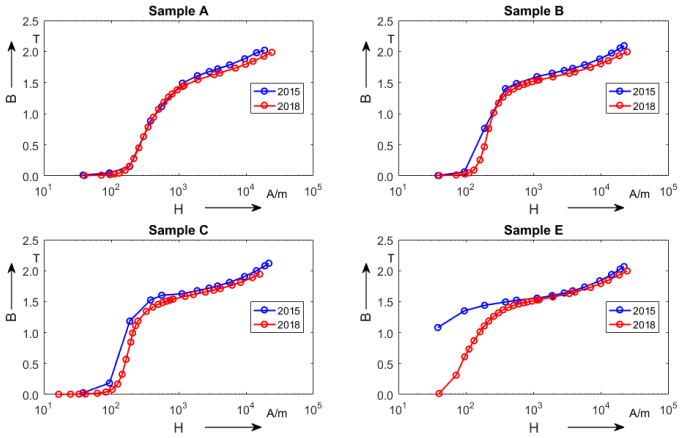

Fig. 5. Difference between the two different campaigns of measurements

E. Effects of cold work on the magnetic properties

A third campaign of measurement was performed on the second batch of samples, whose description is reported in Section III-A. These samples are compatible with the annealing shown by sample B in Fig. 2 of Section III-B. The goal of this third campaign was to verify if the mechanical stress that the material suffers during the production phases could significantly change the material's magnetic properties. For this purpose, the three samples were tested magnetically as delivered from the factory and after the application of a mechanical stress. This consisted of bending the samples along the diameter. In particular, the samples A25112-3 and A25114-4 were bent 6 mm while the sample A25112-4 was bent 4 mm. These tests correspond to the worse case scenario, because even the inner bending radius of a standard coil does not result in such a bending for the material. The magnetic properties of the material before and after the application of the mechanical stress are highlighted in Fig. 6.

In Fig. 7 the comparison before and after the stress for each samples is shown.

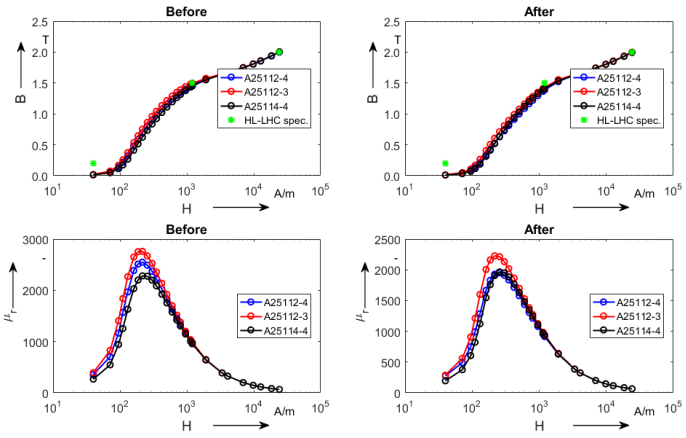

Fig. 6. Measurements performed before and after the application of a mechanical stress to the three samples of the second group of samples

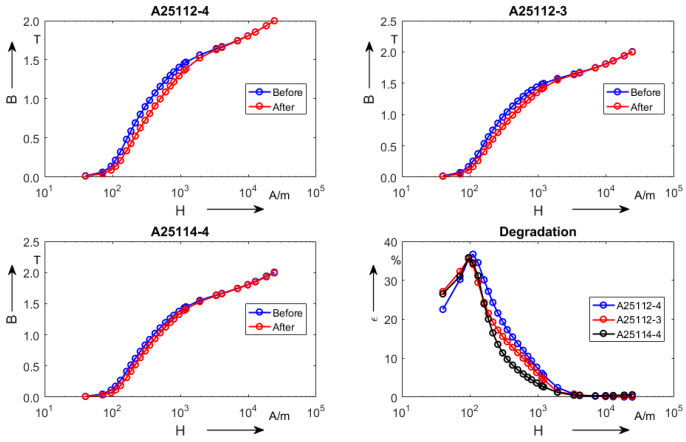

Fig. 7. Comparison between the B-H curves before and after the stress (two figures upper and lower-left) and percentage degrading (lower-right)

After the bending, the magnetic properties are degraded, but in a reproducible way. As shown in the diagram of Fig. 7, the degradations follow the same trend with the maximum value of degradation at low fields. This means that the mechanical stress affects the initial rather than the peak permeability. Moreover, the results confirm the same conclusions reached for the annealing process. The magnetic properties of ARMCO could be optimized by means of an annealing process, which increases the grain size and optimizes the impurity diffusion within the micro-structure. The problem is that the effects of this optimization are easily lost because the material is a pure iron: a little perturbation is enough to modify and lose the effect of the treatment and the more the material is optimized, the higher will be the degradation of its magnetization. This is confirmed by the results in Fig. 6 and Fig. 7: the higher is the permeability peak (samples A25112-3 and A25112-4) and the higher is the degradation of the magnetic properties.

IV. Conclusion

It was demonstrated that annealing enhances the magnetic properties of a pure iron, but this effect is very unstable. It changes at cryogenic temperature or if a mechanical stress is applied. At cryogenic temperatures, the low temperature effects are predominant respect to the effect of the strain. In general, the change in temperature has a larger effect on the magnetic degradation than the mechanical stress. Moreover, this study underlines that the effect of annealing is completely lost after the material is subject to a fast cooling to cryogenic temperatures. Different annealing procedure were used, but without stable results in terms of grain size. Moreover, the annealing generated a surface problem of scaling. For this reason and because the effect of annealing is completely lost after the material is subject to a fast cooling to cryogenic temperatures, the strong annealing phase (initially scheduled) has been removed from the production process for the HL-LHC magnet production. The choice to stop annealing the laminations generated a reduction of roughly 9% of the total costs.

Acknowledgment

The authors would like to thank S. Sgobba for the precious and stimulating discussions about metallurgical procedures and effects of the mechanical strain on the magnetic properties. D. Perini and M. Garlasche for the support to the mechanical tests. R. B. Mercadillo and T. Koettig and S. Prunet for the technical support to the cryogenic permeability measurements.

References

[1] L. Rossi, O. Brüning *et al.*, "High luminosity large hadron collider," in *European Strategy Preparatory Group-Open Symposium, Krakow*, 2012.

[2] L. Bottura, G. de Rijk *et al.*, "Advanced accelerator magnets for upgrading the lhc," *IEEE Transactions on Applied Superconductivity*, vol. 22, no. 3, pp. 4 002 008–4 002 008, 2012.

[3] P. Harlet, F. Beco, and L. Renard, "ProcÃľdÃľ de production d'acier doux," 7 1994, patent EP 0681031A1-B1.

[4] S. Babic, S. Comel *et al.*, "Toward the production of 50 000 tonnes of low-carbon steel sheet for the lhc superconducting dipole and quadrupole magnets," *IEEE Transactions on Applied Superconductivity*, vol. 12, no. 1, pp. 1219–1222, Mar 2002.

[5] F. Bertinelli, S. Comel *et al.*, "Production of low-carbon magnetic steel for the lhc superconducting dipole and quadrupole magnets," *IEEE Transactions on Applied Superconductivity*, vol. 16, no. 2, pp. 1777–1781, June 2006.

[6] P. Ferracin, G. Ambrosio *et al.*, "Development of mqxf: The nb 3 sn low-β quadrupole for the hilumi lhc," *IEEE Transactions on Applied Superconductivity*, vol. 26, no. 4, pp. 1–7, 2016.

[7] F. Savary, E. Barzi *et al.*, "The 11 t dipole for hl-lhc: Status and plan," *IEEE Transactions on Applied Superconductivity*, vol. 26, no. 4, pp. 1–5, 2016.

[8] "Technical specification for the supply of low carbon steel sheets for the superconducting magnets of the hl-lhc," 2015, eDMS No - 1498836.

[9] I.-I. E. Commission *et al.*, "Magnetic materials-part 4: Methods of measurement of dc magnetic properties of magnetically soft materials," 2000.

[10] P. Arpaia, A. Liccardo *et al.*, "On the use of fluxmetric methods for characterizing feebly magnetic materials," in *2017 IEEE International Instrumentation and Measurement Technology Conference (I2MTC)*, May 2017, pp. 1–6.

[11] M. KÃijpferling, C. Appino *et al.*, "Magnetic hysteresis in plastically deformed low-carbon steel laminations," *Journal of Magnetism and Magnetic Materials*, vol. 316, no. 2, pp. e854 – e857, 2007, proceedings of the Joint European Magnetic Symposia.

[12] E. Ferrara, E. Olivetti *et al.*, "Microstructure and magnetic properties of pure iron for cyclotron electromagnets," *Journal of Alloys and Compounds*, vol. 615, pp. S291 – S295, 2014, sI :ISMANAM 2013.